JOURNAL OF MATERIALS SCIENCE **40** (2005) 4469–4473

Novel quantitative method for evaluation pitting corrosion and pitting corrosion inhibition of carbon steel using electrochemical noise analysis

X. P. GUO*, Z. Y. CHEN, JUNÈ QU, Z. H. DONG
Department of Chemistry,Huazhong University of Science and Technology, Wuhan, 430074 China
E-mail: guoxp@mail.hust.edu.cn

The electrochemical noise of N80 steel in sodium chloride solution containing 0.5 M bicarbonate with and without inhibitor was recorded. The current signal which corresponded to pitting corrosion was extracted from the records based on wavelet transform, then the intergraded current was calculated. Comparing with the intergraded current with and without inhibitor, the inhibition efficiency on pitting corrosion was calculated. Electrochemical impedance spectroscopy (EIS) measurements were also done to validate the electrochemical noise analysis results. From this paper, it was shown that pitting corrosion and inhibition efficiency on pitting corrosion could be evaluated accurately and quantitatively through intergrading pitting corrosion current which extracted based on wavelet transform.

1. Introduction

Electrochemical noise (ECN) measurement has many advantages over other electrochemical techniques, including low cost of the equipment, ease of data collection, non-disturbance on system [1], sensitivity to localized corrosion processes and capability of predicting pitting corrosion initiation [2]. In our laboratory the inhibition of CrO_4^{2-} and MoO_4^{2-} ions on carbon steel pitting corrosion has been studied through intergraded current using ECN [3], but since other kinds of noise was also contained in the records, there must be some error when this method was applied directly to evaluate pitting corrosion and inhibition efficiency on pitting corrosion, especially when the data is from filed recording. In order to evaluate accurately pitting corrosion or inhibition efficiency on pitting corrosion, the signal that corresponds to pitting corrosion must be extracted from the records.

Since noise corresponding to pitting corrosion has its own characteristic frequency range [4], the noise that corresponds to pitting corrosion can be extracted from the recordings through proper method. After the extraction, the intergraded current of the pitting corrosion noise can be calculated.

Wavelet transform is a new signal processing tool, it developed very quickly during the last 20 years. The primary attractive feature of wavelet transform is its capacity for multi-resolution analysis, which makes it suitable for non-stationary signal processing. With wavelet transform, signal component can be extracted from a noisy signal without appreciable degradation [5–7].

The aim of this study is to bring forward a new method to evaluate quantitatively pitting corrosion and inhibition efficiency on pitting corrosion more accurately, the method was validated by some recording data.

2. Signal decomposition by wavelet transform

The wavelet transform of signal $f(t)$ is defined as [8]

$$(W\psi f)(b,a) = |a|^{-1/2} \int_{-\infty}^{+\infty} f(t)\bar{\psi}\left(\frac{t-b}{a}\right) dt \quad (1)$$

where ψ is named mother wavelet or basic wavelet and $\bar{\psi}$ is the complex conjugate of ψ

Let

$$\psi_{ab}(t) = |a|^{-1/2}\,\psi\left(\frac{t-b}{a}\right) \quad (2)$$

then, ψ_{ab} is the wavelet bases. The parameter a characterizes the frequency of $f(t)$ and is named scale, while the parameter b characterizes the position of $f(t)$ in time or space.

The discrete wavelet transform (DWT) is more efficient for discrete time signals [9]. The most commonly

* Author to whom all correspondence should be addressed.
0022-2461
DOI: 10.1007/s10853-005-0924-0

used discrete wavelet transform is the scaling and shifting of parameters with powers of two, i.e., $a = 2^j$, $b = k2^j$ with $j, k \in Z$, where j is the number of levels in the discrete wavelet transform. The empirical wavelet coefficients $C_{j,k}$ are found by projecting the signal $f(t)$ onto the wavelet basis set $\psi_{j,k}(t)$ i.e.

$$C_{j,k} = \langle f(t), \psi_{j,k} \rangle \tag{3}$$

At each level j, a deviation signal called the j-level detail $D_j(t)$ can be calculated according to the following equations:

$$D_j(t) = \sum_{k \in z} C(j,k)\psi_{j,k}(t), \quad j, \quad k \in Z \tag{4}$$

At a reference level J, the following equation is valid:

$$f(t) = \sum_{j=1}^{J} D_j(t) + A_J(t) \tag{5}$$

Where $A_J(t)$ is defined as an approximation of signal $f(t)$ and associated with indices $j \leq J$ by the following equation:

$$A_J(t) = \sum_{j>J} D_j(t) \tag{6}$$

In this work, the symlets wavelets were selected considering the boundary conditions and orthogonality [11].

3. Experimental

3.1. Materials and solutions

Cylindrical specimens were made from a sheet of N80 steel (composition given in Table I) as working electrodes. The electrodes were coated by epoxy resin only leaving one flat face with and area of 1 cm^2 exposed to the solution, then the surface was polished with SiC paper up to 1200 grit, washing with distilled water, degreased with acetone, and drying in air.

All the solutions were prepared from analytical grade reagents and distilled water.

3.2. Experimental procedures

Electrochemical noise measurements were performed in a three-electrode setup, allowing simultaneous recording of current and potential noise. Two identical working electrodes were immersed in the test solution at 35°C, the current noise between the above two nominally identical working electrodes was obtained using a zero resistance (ZRA, current sensitivity >10 pA) measurement system at a sampling frequency $fs = 2$ Hz. The measurement system ensures the necessary amplification (ICL7650) of measured signals and a high accuracy $\sum - \delta$ 20 bit A/D converter (AD 7703) was used in the design, an anti-aliasing low pass filter was applied before the A/D conversion.

Electrochemical impedance spectroscopy (EIS) measurements were carried out by IM6e Impedance Measurement system manufactured by Zahner elektrik company, German. A Pt plate and a saturated calomel (SCE) were used as the counter electrode and reference electrode, respectively. All impedance measurements were performed at open circuit potential with amplitude of 10 mV in the frequency range about 10 mHz to 5 kHz.

TABLE I The chemical composition of N80 steel

C	Mn	P	S	Cr	Mo	Ni	Fe
0.24	1.19	0.013	0.004	0.036	0.021	0.028	Remainder

4. Results and discussion

4.1. ECN in 0.5 $MNaHCO_3$ solution with different concentration of Cl^-

After being pre-passive in 0.5 $MNaHCO_3$ for 30 minutes, the two working electrodes were then immersed in the test solution. Fig. 1 shows the experimental current vs. time plots which correspond to N80 steel after 20 minutes of immersion in 0.5 $MNaHCO_3$ with different NaCl concentrations, namely 0.2, 0.4 and 0.6 M.

It can be observed form Fig. 1 that when the concentration of Cl^- is 0.2 M, the noise which corresponds to pitting corrosion was not prominent, there was mainly high frequency noise with small amplitude which corresponds to general corrosion, when the concentration of Cl^- reached 0.4 M, the current noise that corresponds to pitting corrosion was very prominent, but when the concentration of Cl^- increased up to 0.6 M, there were only few current transients which correspond to pitting corrosion, the corrosion behavior was mainly the active dissolution of the corrosion film.

In order to evaluate pitting corrosion, the current noise corresponding to pitting corrosion should be extracted from the recordings. In order to extract the current signal corresponding to pitting corrosion, the characteristic frequency corresponding to pitting corrosion is firstly found out by so-called power distribution fraction (PDF) [10, 11]. The power distribution fraction of level j is defined as

$$E_j^d = D_j^2(t)/E \tag{7}$$

$D_j(t)$ can be calculated according to Equation 4 based on wavelet transform and E which is the total energy of the ECN is calculated according to the following equation:

$$E = \sum_{n=1}^{n} x_n^2 \quad n = 1, \ldots, N \tag{8}$$

where $x_n (n = 1, \ldots, N)$ is the element of ECN, N is the total number of the elements.

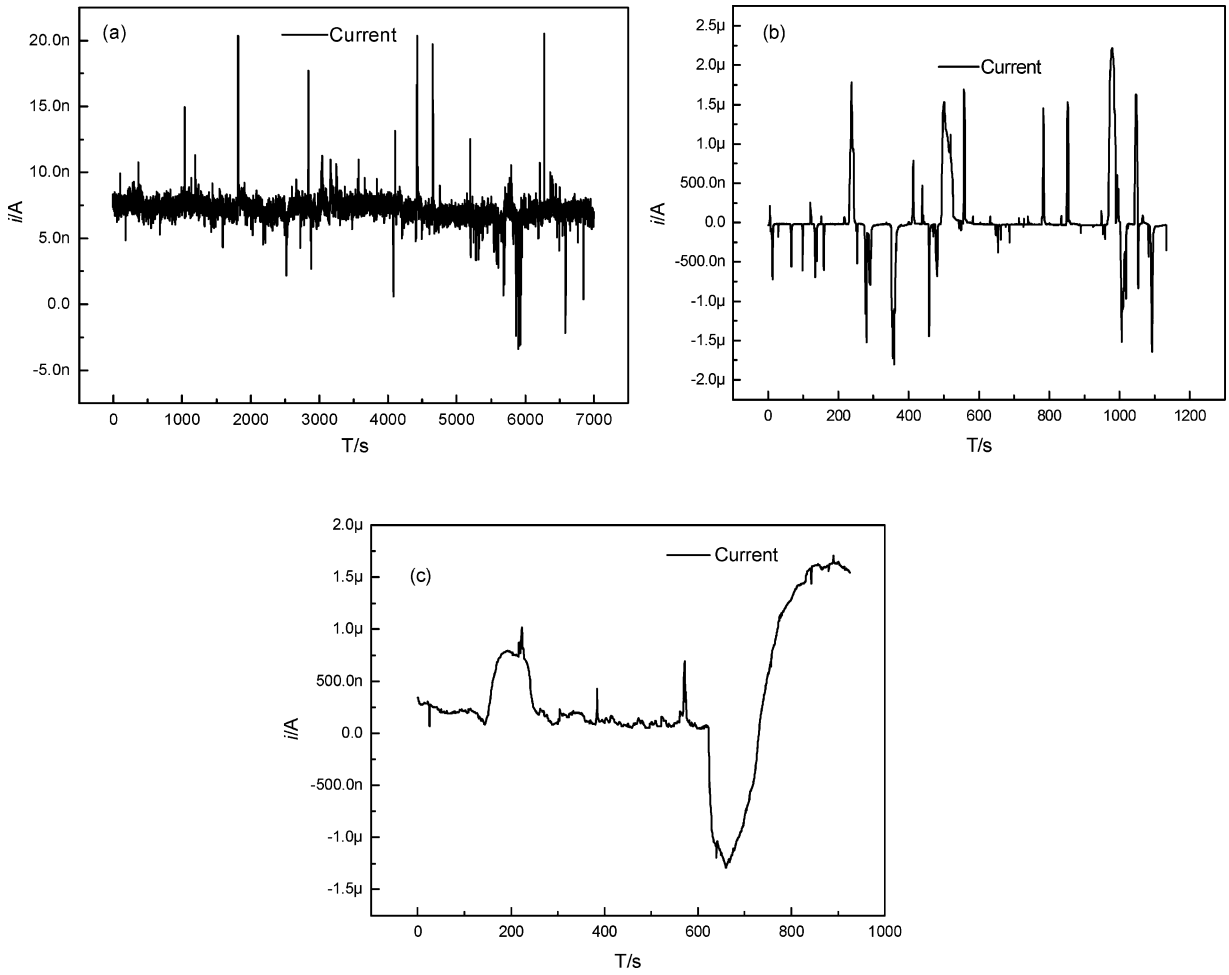

Figure 1 ECN corresponds to N80 steel in 0.5 $MNaHCO_3$ with different concentrations of NaCl. (a) 0.2 M, (b) 0.4 M, and (c) 0.6 M.

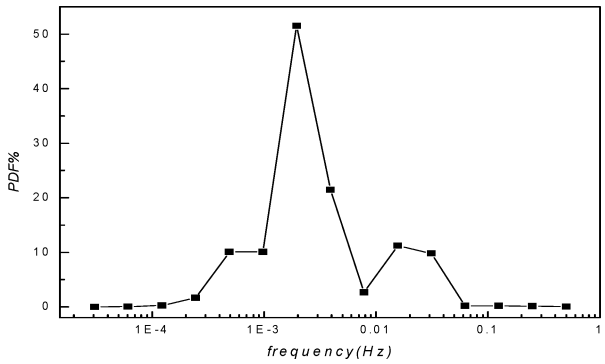

Figure 2 PDF vs. log frequency corresponding to ECN shown in Fig. 1c.

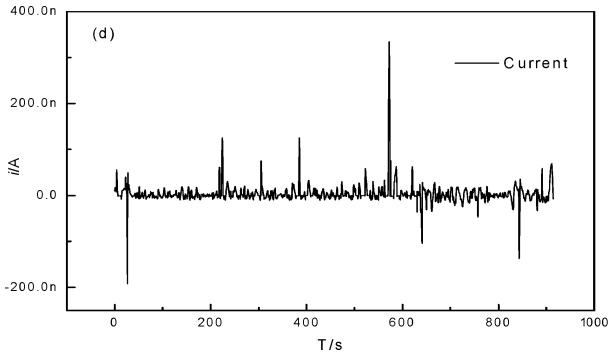

Figure 3 Current signal corresponding to pitting corrosion extracted from ECN showed in Fig. 1c.

The frequency range of level j is $fs/2/2^j \sim fs/2/2^{j-1}$, where fs is the sampling rate.

Fig. 2 shows the curve of PDF vs. log frequency corresponding to ECN shown in Fig. 1c.

The PDF plot turns out that the energy of the ECN showed in Fig. 1c is stored predominantly around 3×10^{-3} Hz, from the character of ECN in Fig. 1c, we know it corresponds to the active solution of the corrosion film, and there is also some peaks with relatively high energy distribution at frequency range from 0.8×10^{-2} to 3×10^{-2} Hz, this part is proven to correspond to pitting corrosion by our previous work [10, 12]. Because the frequency range of level j corresponds to $fs/2/2^j \sim fs/2/2^{j-1}$, the power distribution fraction j that relate to pitting corrosion is from 6 to 7.

Then the current signal corresponding to pitting corrosion was extracted from the recording based on Equations 4 and 5. Fig. 3 shows the extracted current signal corresponding to pitting corrosion of N80 steel in 0.5 $MNaHCO_3$ + 0.4 MNaCl.

The current signal corresponding to pitting corrosion of N80 steel in 0.5 $MNaHCO_3$ solution with 0.2 M and 0.4 MNaCl was also extracted from the recordings based on wavelet transform.

The charge of the current transients Q_{pit} corresponding to pitting corrosion was calculated by the following

TABLE II Parameters of ECN corresponding to pitting corrosion

	Nucleation rate (s^{-1})	Mean amplitude (μA)	Mean life (s)	Integrated current per hour (C/h)
0.5 $MNaHCO_3$ + 0.2 MNaCl	0.016	0.011	11.3	2.84e-6
0.5 $MNaHCO_3$ + 0.4 MNaCl	0.053	0.926	18.2	0.0011
0.5 $MNaHCO_3$ + 0.6MNaCl	0.0089	0.32	22.1	1.07e-4

equation [13]:

$$Q_{\text{pit}} = \frac{3600}{T} \sum_{t=0}^{T} (|i(t)| \times \Delta t) \tag{9}$$

Where T is the measurement time (in seconds), $i(t)$ is the current signal that corresponds to pitting corrosion extracted from the recording, Δt is the sampling interval.

The nucleation rate of the pit, mean amplitude and mean life of the current transients were also calculated [12], the results were summarized in Table II.

It can be observed from Table II that the pitting corrosion of N80 steel became more serious when the Cl^- concentration increased from 0.2 to 0.4 M, but once the Cl^- concentration reached 0.6 M, since the active dissolution of the passive film became the predominated corrosion behavior, the pitting corrosion was weakened.

4.2. ECN in 0.5 M $NaHCO_3$ + 0.4 MNaCl with inhibitor

After being pre-passive in 0.5 $MNaHCO_3$ solution for 30 min, the working electrodes were then immersed in 0.5 $MNaHCO_3$ + 0.4 MNaCl. Inhibitor was dropped after observing obvious noise transients. Fig. 4 shows the experimental current vs. time plots after 20 min of the addition of 0.1 $MMoO_4^{2-}$.

Then the PDF of the current noise showed in Fig. 4 was calculated and shown in Fig. 5.

It can be observed from Fig. 5 that there is a maximum peak at frequency about 10^{-4} Hz, which corresponds to the low frequency drift of the current noise in Fig. 4, and there is also some peaks with relatively higher power distribution with the frequency range

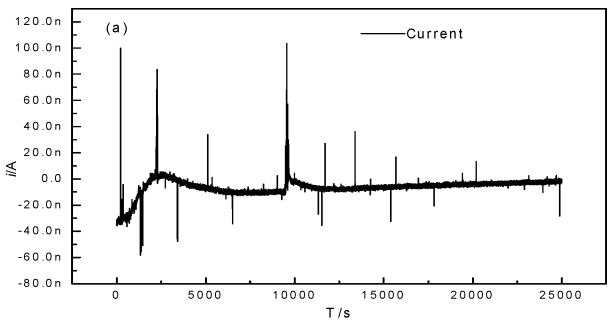

Figure 4 ECN corresponding to N80 steel in 0.5 $MNaHCO_3$ + 0.4 NaCl + 0.1 $MMoO_4^{2-}$.

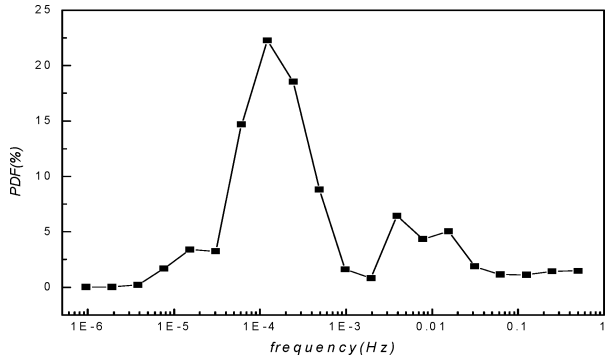

Figure 5 PDF vs. log frequency corresponding to ECN shown in Fig. 4.

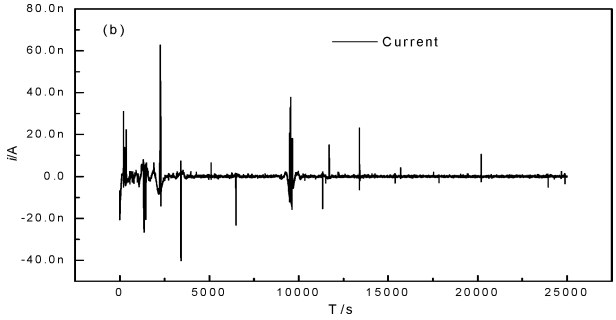

Figure 6 Current signal corresponding to pitting corrosion extracted from ECN showed in Fig. 4.

from 0.3×10^{-2} to 3×10^{-2} Hz, which corresponds to pitting corrosion. Fig. 6 shows the current signal that corresponds to pitting corrosion extracted from the recording showed in Fig. 4.

The current signal corresponding to pitting corrosion of N80 steel in 0.5 $MNaHCO_3$ + 0.4 MNaCl with 0.02 $MMoO_4^{2-}$ and 0.05 $MMoO_4^{2-}$ was also extracted from the records based on wavelet transform.

Then the integrated current within one hour was calculated, and the inhibition efficiency on pitting corrosion was also calculated according to following equation [3]:

$$\eta = \left(\frac{Q_b - Q_h}{Q_b} \right) \times 100\% \tag{11}$$

where Q_b and Q_h are the integrated current within one hour corresponding to pitting corrosion in presence and absence of inhibitor respectively. Some other parameters of ECN were also calculated and summarized in Table III.

It can be observed form Table III that the pit nucleation rate, average current amplitude and lifetime of current transient, integrated current decreased with the addition of MoO_4^{2-}, they still decreased with increasing MoO_4^{2-} concentrations, and the inhibition efficiency on pitting corrosion of MoO_4^{2-} increased with increasing MoO_4^{2-} concentrations.

4.3. EIS

Fig. 7 shows the impedance spectra for N80 steel in 0.5 $MNaHCO_3$, 0.5 $MNaHCO_3$ + 0.4 NaCl and 0.5

TABLE III Parameters of ECN corresponding to pitting corrosion

	Nucleation rate (s^{-1})	Avergage amplitude (μA)	Averge lifetime (s)	Integrated current per hour (C/h)	Inhibition efficiency (%)
0.5 $MNaHCO_3$ + 0.4 MNaCl	0.053	9.26e-7	18.20	0.0011	–
0.5 $MNaHCO_3$ + 0.4 MNaCl + 0.02 $MMoO_4^{2-}$	0.044	7.04e-7	15.62	9.12e-4	17.10
0.5 $MNaHCO_3$ + 0.4 MNaCl + 0.05 $MMoO_4^{2-}$	0.026	3.54e-7	9.334	1.35e-4	87.73
0.5 $MNaHCO_3$ + 0.4 MNaCl + 0.10 $MMoO_4^{2-}$	0.0038	2.13e-8	6.84	3.90e-6	99.65

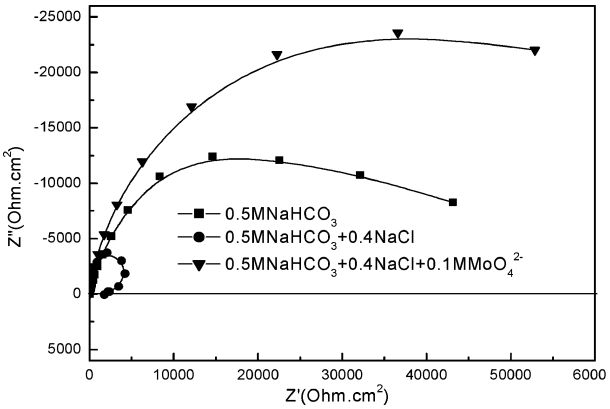

Figure 7 Nyquist plots for N80 electrodes exposed to different solution at 35°C.

$MNaHCO_3$ + 0.4 NaCl + 0.1 $MMoO_4^{2-}$, respectively at open circuit potential. The Nyquist plot corresponding to N80 electrode in 0.5 $MNaHCO_3$ solution shows two capacitive semicircles at high and at low frequencies, respectively. But when the electrode was in 0.5 $MNaHCO_3$ + 0.4 NaCl, the Nyquist diagram consists of a capacitive loop in high frequency and an inductive loop in low frequency, and the diameter of high frequency capacitive semicircle sharply reduced, which indicate the initiation of pitting corrosion [13]. After the addition of inhibitor MoO_4^{2-}, the inductive component was disappeared and the impedance module increased largely, which indicates that the electrode gets into stage of passivity again.

5. Conclusions

Intergraded current based on wavelet transform can evaluate pitting corrosion and pitting corrosion inhibition quantitatively, since it eliminates disturbance of other noise, the pitting corrosion and pitting corrosion inhibition can be evaluated more accurately. In this study, intergraded current based on wavelet transform has been used to study the pitting corrosion of N80 steel exposed to sodium chloride solution with and without inhibitor. It was known from the research that the pitting corrosion of N80 steel was more severe with the increase of Cl^- concentration from 0.2 to 0.4 M, but it then decreased when Cl^- concentration reached 0.6 M. MoO_4^{2-} has obvious inhibition effect on N80 pitting corrosion and the inhibition efficiency increased with increasing MoO_4^{2-} concentrations.

References

1. A. ABALLE, M. BETHENCOURT, F. J. BOTANA and M. MARCOS, *Rev. Metal* **1** (1998) 42.
2. C. N. CAO and X. Y. CHANG, *Chinese Society of Corrosion and Protection* **1** (1989) 21.
3. Z. H. DONG and X. P. GUO, *Journal of Applied Electrochemistry* **4** (2002) 395.
4. S. JANUSZ and D. KAZIMIERZ, *Eletrochemistry Communications* **4** (2002) 388.
5. S. MALLAT, A Wavelet Tour of Signal Processing (Academic Press, 1999) p. 56.
6. Y. J. ZHENG, B. H. DAVID and L. M. LI, *Signal Processing* **8** (2000) 1535.
7. Z. Y. CHEN and X. P. GUO, *Shandong Journal of Biomedical Engineering* **3** (2002) 29.
8. A. GROSSMANN and J. MORLET, *SIAM J. Math. Anal.* **4** (1984) 4.
9. S. G. MALLAT, *IEEE Transactions on Pattern Analysis and Machine Intelligence* **6** (1989) 674.
10. Z. H. DONG and X. P. GUO, *Electrochemistry Communications* **3** (2001) 561.
11. A. ABALLE, M. BETHENCOURT, F. J. BOTANA and M. MARCOS, *Electrochimica Acta* **26** (1999) 4805.
12. Z. Y. CHEN and X. P. GUO, in The 8th Youth Corrosion Conference of China, Wuhan, April 2003, edited by China Society for Corrosion and Protection, p. 78.
13. H. Y. YANG, J. J. CHEN, C. N. CAO and D. Z. CAO, *Journal of Chinese Society for Corrosion and Protection* **5** (2000) 287.

Received 27 August 2004
and accepted 14 March 2005